Noise estimation from digital step-model signal

Olivier LALIGANT, Frédéric TRUCHETET, Eric FAUVET

Le2i Lab., CNRS UMR 6306, Université de Bourgogne

12 rue de la Fonderie, 71200 Le Creusot, France

olivier.laligant@u-bourgogne.fr

Abstract—This paper addresses the noise estimation in the digital domain and proposes a noise estimator based on the step signal model. It is efficient for any distribution of noise because it does not rely only on the smallest amplitudes in the signal or image. The proposed approach uses polarized/directional derivatives and a nonlinear combination of these derivatives to estimate the noise distribution (e.g., Gaussian, Poisson, speckle, etc.). The moments of this measured distribution can be computed and are also calculated theoretically on the basis of noise distribution models. The 1D performances are detailed, and as our work is mostly dedicated to image processing, a 2D extension is proposed. The 2D performances for several noise distributions and noise models are presented and are compared to selected other methods.

Index Terms—Noise estimation, noise estimator, step model, edge model, digital signal, noise distribution, Gaussian white noise, impulse noise, salt and pepper noise, Poisson noise, nonlinear model, multiplicative noise, CCD sensor

I. INTRODUCTION

Noise is omnipresent in signals produced or transmitted by real devices and most signal- and image-processing techniques take (or should take) noise into account to obtain efficient results. Data compression, pattern recognition, and 3D reconstruction are examples in which it is essential to know the noise level and, if possible, the noise distribution.

Certain works specifically address the problem of noise estimation by primarily assuming the noise to be white and additive. Filtering methods use cleaning filters (mean, median) and measure the noise using the difference between noisy and restored images [22]. The contribution of the pixels is controlled by the gradient intensity (the contribution is null for high gradient locations and for edges). Canny estimated the noise from the lower 80th percentile in the gradient modulus histogram of the edge response of his filter [3]. For Gaussian white noise, Bracho and Sanderson [1] observed that the noise gradient modulus is Rayleigh-distributed, and a distribution fit leads to a standard deviation corresponding to the histogram mode that is not strongly affected by edge gradients. Vorhess and Poggio [32] improved this approach by considering only the steepest part of the distribution that essentially contains most of the noise. Several approaches to variance estimation are block-based, and either the size of the blocks is fixed (size 5×5 [16], 7×7 or 8×8) or is variable, as in a multiresolution pyramid; in the latter case, a sophisticated selection algorithm is required [20]. A survey of the majority of the previously cited methods can be found in [22]. The general conclusion can be drawn that the simple average- and median-based methods perform better than the block-based methods. In [26],

noise estimation for color images is proposed based on the statistical prior knowledge that signal information is highly correlated between the channels. Another interesting work on noise estimation focuses on the camera CCD response [18], [17].

Wavelet-based methods for the estimation of noise are promising. De Stefano *et al.* [28] proposed three methods that use wavelet decomposition of the image and a training approach. Improvements in the gradient approach are based on the Laplacian [9] and adaptive edge detection [29]. More complex methods are proposed, such as that in [34], in which the scale and orientation models for the structure allow for noise and signal separation, and in [10] for noise estimation in remote sensing via marginalized likelihood maximization. The MAD estimator introduced by Donoho and Johnstone [7], [6] is one of the most commonly used estimators, most likely due to its efficiency and simplicity.

Noise estimate is often involved in signal and image de-noising methods. De-noising methods often require a noise estimate parameter or are based on a tradeoff between a noisy solution and a smoothing solution in an iterative strategy as proposed in [24], [15]. Those methods are dense because all points must be restored. Therefore, the noise component cannot always be clearly separated from the signal (due to the tradeoff required in the solution). Methods that operate in the spatial domain are essentially based on linear or nonlinear filters (median, SUSAN [25], bilateral filtering [30]) and anisotropic diffusion [23], [31]. The introduction of the wavelet and sparse theory has led to the development of transform domain methods [6], [27], [12], [33], [19] that were primarily based on the frequency approach. Reviews of a portion of these de-noising methods can be found in [2], [21].

In this work, we propose the use of polarized first derivatives to define a noise estimator. We introduced such derivatives in [13] as a means of obtaining a new method for edge detection in images, and this method presents interesting properties that are applicable to both edge localization and noise reduction.

The proposed noise estimator is based on the step signal model. However, the proposed approach is able to deal with any noise distribution and with any relationship between the noise and the signal. The polarized derivatives lead to measurements of the distribution of the noise based on the separation of impulse components from the step signal. The corresponding random variable is modeled, its probability distribution function is calculated and the first statistical moments are expressed in terms of the noise parameters (e.g., the

variance of a Gaussian additive noise). From this distribution, an estimator is then defined to produce an estimate of the main noise parameter. Notably, this method is able to take advantage of the polarized derivatives to estimate the asymmetry of the noise distribution. Theoretically, it is even possible to deduce the noise distribution from the measured distribution.

The organization of this paper is as follows: the principle of noise extraction is introduced in Section II followed by the definition of the noise estimator in Section III. The performance of the model for 1D signals is studied in Section IV. In SectionV, a 2D extension and selected results are proposed: this section is completed by a discussion of the limitations of the proposed approach. Summary perspectives conclude this work, and certain technical and complementary details regarding the proposed approach can be found in the supplemental report [14].

II. Noise extraction

This section introduces the selected signal and noise definitions, the new derivative operators and, finally, the noise measures. These measures will be used in Section III to define the noise estimator.

A. Notations and definitions

We denote the following:

x_k is the noisy digital signal at the instant (or the position) k;

n_k is the noise outcome at the instant or the position k and N_k is the corresponding random variable;

P_{N_k} is the probability density function (*pdf*) of N_k;

σ is the standard deviation and $v = \sigma^2$ the variance of the noise distribution of N_k (in the case of an additive GWN or Gaussian White Noise, σ is the parameter of the *pdf*). The signal model is assumed as the step function:

$$x_k = AH_k + n_k \tag{1}$$

where H_k is the Heaviside function: $H_k = 1$ if $k \geq 0$, 0 elsewhere, and A is the amplitude.

We now introduce the following polarized and oriented differentiating components:

$$\begin{cases} y_k^{R+} = T(x_{k+1} - x_k) \\ y_k^{R-} = -T[-(x_{k+1} - x_k)] \\ y_k^{L+} = T(x_k - x_{k-1}) \\ y_k^{L-} = -T[-(x_k - x_{k-1})] \end{cases} \tag{2}$$

where T is a nonlinear threshold operator: in this work $T(u) = u$ if $u \geq 0$, 0 elsewhere. Simplifying the notations with the polarized and oriented derivative operators $D^{R+}, D^{L+} : \mathbb{R} \to \mathbb{R}^+$, $D^{R-}, D^{L-} : \mathbb{R} \to \mathbb{R}^-$, the components are now written as:

$$\begin{cases} y^{L+} = D^{L+}(x) & y^{R+} = D^{R+}(x) \\ y^{L-} = D^{L-}(x) & y^{R-} = D^{R-}(x) \end{cases} \tag{3}$$

In the next sections, we demonstrate how to construct a noise estimator based on these components. We introduce the signal decomposition into the derivative components to produce a noise extraction from these components.
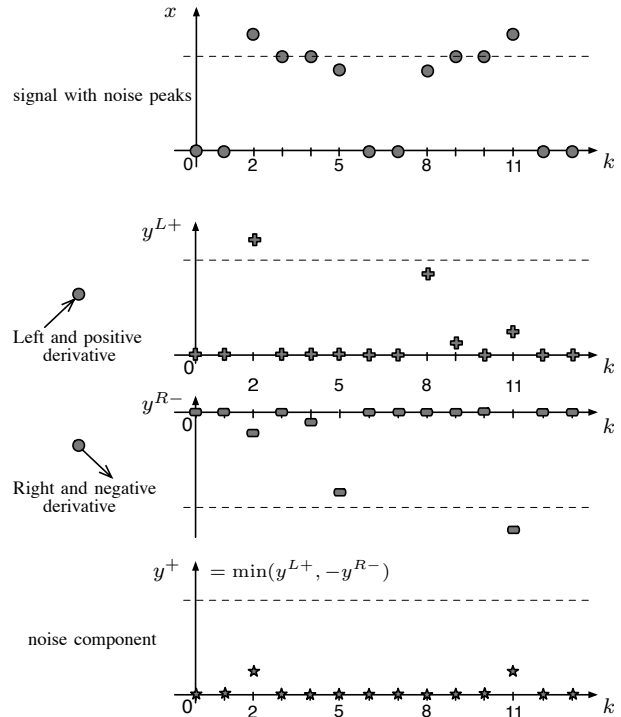

Figure 1. The signal x is assumed to be a sum of four elementary step signals and four noise peaks (at $k \in \{2, 5, 8, 11\}$) or two elementary step signals (at $k \in \{2, 11\}$), two smooth (aliased) steps (at $k \in \{5, 8\}$) and only two noise peaks (at $k \in \{2, 11\}$). Polarized and oriented detections: y^{L+} and y^{R-}. The nonlinear derivative y^{L+} detects the positive (and noisy) steps and positive peaks. In the same way, y^{R-} gives the negative (and noisy) steps and peaks. $y^+ = \min\left(y^{L+}, -y^{R-}\right)$ gives the peak noise values at $k = 2$ and $k = 11$.

B. Signal decomposition

Let us consider the operators D^{L+} and D^{R-} and a somewhat realistic signal x as shown in Figure 1. Applying these operators, we obtain y^{L+} and y^{R-}. At the current abscissa k, y^{L+} corresponds to a left-hand derivative on positive slopes (defined on the abscissas $k-1$ and k). It follows that y^{L+} has only non-zero values for $k \in \{2, 8, 9, 11\}$. y^{R-} is the right-hand derivative on negative slopes (defined on the abscissas k and $k+1$) leading to non-zero values for $k \in \{2, 4, 5, 11\}$. The signal x in Figure 1 can be seen as the sum of four elementary step signals and a noise signal n_k presenting non-zero values at the positions $\{2, 5, 8, 11\}$. Another interpretation of the signal is as follows: two elementary step signals (at $k \in \{2, 11\}$) and two smooth (aliased) steps (at $k \in \{5, 8\}$) and only two noise peaks (at $k \in \{2, 11\}$).

Inverting x leads to a similar analysis for D^{L-} and D^{R+}: see Figure 2.

C. Noise measures

From the signals in the above section, we propose a definition of the noise measures:

$$\begin{cases} y^+ = \min\left(y^{L+}, -y^{R-}\right) \\ y^- = -\min\left(-y^{L-}, y^{R+}\right) \end{cases} \tag{4}$$

We focus now on y^+ knowing that the same considerations can be drawn for y^-. In the example of Figure 1, $y_2^+ = -y_2^{R-}$,
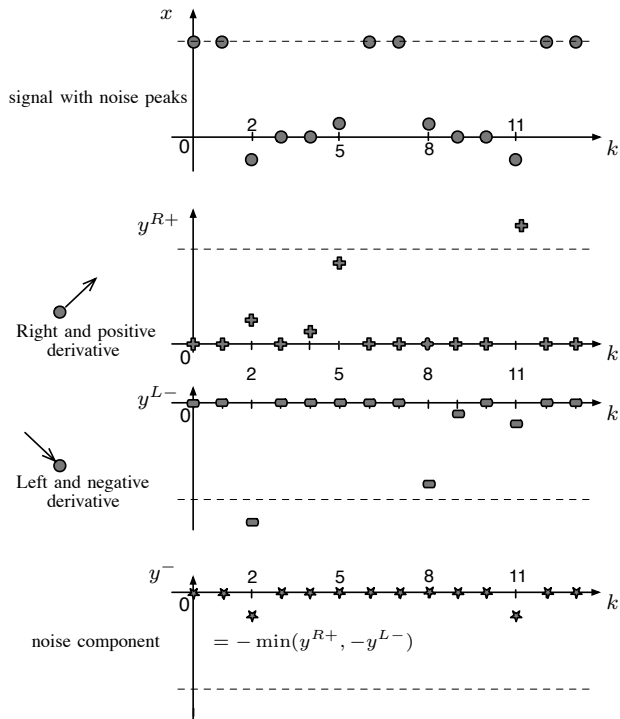
2

Figure 2. The signal x is an inverted version of Figure 1. It is assumed to be a sum of four elementary step signals and four noise peaks (at $k \in \{2, 5, 8, 11\}$) or two elementary step signals (at $k \in \{2, 11\}$), two smooth (aliased) steps (at $k \in \{5, 8\}$) and only two noise peaks (at $k \in \{2, 11\}$). Polarized and oriented detections: y^{R+} and y^{L-} and finally $y^- = -\min\left(y^{R+}, -y^{L-}\right)$. y^- also contains two peaks of noise.

$y_{11}^+ = y_{11}^{L+}$, elsewhere $y_k^+ = 0$. This example shows that y^+ contains a part of the noise of the original signal x. Considering the second assumption on x (aliasing of the two steps at $k \in \{5, 8\}$), y^+ is the noise signal.

Whatever the assumption on x, the components of y^+ are:

$$y_k^{L+} = \begin{cases} x_k - x_{k-1} & \text{if } x_k \geq x_{k-1} \\ 0 & \text{elsewhere} \end{cases} \quad (5)$$

$$y_k^{R-} = \begin{cases} 0 & \text{if } x_{k+1} > x_k \\ x_{k+1} - x_k & \text{elsewhere} \end{cases} \quad (6)$$

and we have the following:

$$y_k^+ = \begin{cases} 0 & \text{if } x_{k-1} \leq x_k < x_{k+1} \\ \min\left(x_k - x_{k-1}, x_k - x_{k+1}\right) & \text{if } x_{k-1} \leq x_k \geq x_{k+1} \\ 0 & \text{if } x_{k-1} > x_k < x_{k+1} \\ 0 & \text{if } x_{k-1} > x_k \geq x_{k+1} \end{cases} \quad (7)$$

y_k^+ is always positive or null ($y_k^+ \geq 0$). Introducing the noisy step model, y^+ becomes for $k \notin \{-1, 0, 1\}$:

$$y_k^+ = \begin{cases} \min\left(n_k - n_{k-1}, n_k - n_{k+1}\right) & \text{if } n_{k-1} \leq n_k \geq n_{k+1} \\ 0 & \text{elsewhere} \end{cases} \quad (8)$$

or:

$$y_k^+ = \begin{cases} n_k - \max\left(n_{k-1}, n_{k+1}\right) & \text{if } n_{k-1} \leq n_k \geq n_{k+1} \\ 0 & \text{elsewhere} \end{cases} \quad (9)$$

For $k \in \{-1, 0, 1\}$, the amplitude A appears in the equation and can bias the noise estimation. A detailed analysis of the influence of A can be found in [14]. The influence on the estimator is quantified in Section IV-B.

y^+ leads to extraction of the positive part of the noise signal while y^- corresponds to the negative part. These two signals are useful for analyzing asymmetric pdf.

III. THE NOISE ESTIMATOR $NOLSE$ (NONLINEAR NOISE ESTIMATOR)

From these noise measures, it is now possible to define a new noise estimator. Assuming the original noise model as known, the probability density function of these measures is defined to allow for the deduction of the variance estimator (and other moments) of the original noise distribution. The *Matlab-Octave* code of the estimator is given in the report [14].

A. Probability density function (pdf) of the measures

We are interested in the pdf associated with the noise measures (e.g. y^+). We have:

$$y_k^+ = \begin{cases} n_k - \max\left(n_{k-1}, n_{k+1}\right) & \text{if } n_{k-1} \leq n_k \geq n_{k+1} \\ 0 & \text{elsewhere} \end{cases} \quad (10)$$

We introduce the probability function P_{N_k} of the random variable N_k in which the outcomes are n_k. Considering the composed variable M corresponding to $\max\left(n_{k-1}, n_{k+1}\right)$, the pdf, if n_{k-1} and n_{k+1} are independent for a study of point correlation, is as follows:

$$\begin{aligned} P_M(v) &= P_{N_{k-1}}(v)P_{N_{k+1}}(N_{k+1} < v) \\ &\quad + P_{N_{k-1}}(N_{k-1} < v)P_{N_{k+1}}(v) \\ &= 2P_{N_{k-1}}(v)\int_{-\infty}^{v} P_{N_{k+1}}(u)du \\ &= 2P_{N_{k+1}}(v)\int_{-\infty}^{v} P_{N_{k-1}}(u)du \end{aligned}$$

We now define the conditional probability P_{Y_k} of the random variable Y_k where the outcomes are $n_k - \max\left(n_{k-1}, n_{k+1}\right)$ with the condition $n_{k-1} \leq n_k \geq n_{k+1}$. The condition means that the events in the variable Y_k are not independent. Nevertheless, it can be simplified as follows:

$$n_k \geq max(n_{k-1}, n_{k+1}) \quad (11)$$

implying that $y_k^+ \geq 0$. Taking into account this result, the composed variable can be written as:

$$Y_k = N_k - M | Y_k \geq 0 \quad (12)$$

meaning that this variable exists only for positive values ($Y_k \geq 0$). The probability function P_{Y_k} can then be deduced by convolution ($y = n - m$):

$$\begin{aligned} P_{Y_k}(y \geq 0) &= \int_{-\infty}^{\infty} P_{N_k}(n)P_M(n - y)dn \\ &= 2\int_{-\infty}^{\infty} P_{N_k}(n)P_{N_{k+1}}(n - y)dn \\ &\quad \times \int_{-\infty}^{n-y} P_{N_{k-1}}(x)dx \end{aligned}$$

3

Knowing the process that generates the noise can be considered as location-independent, we finally have

$$P_{Y_k}(y \geq 0) = 2 \int_{-\infty}^{\infty} P_{N_k}(n) P_{N_k}(n-y) dn \int_{-\infty}^{n-y} P_{N_k}(x) dx \tag{13}$$

The mean and second moment are then described by

$$E[Y_k] = \int_0^{\infty} y P_{Y_k}(y) dy \tag{14}$$

$$E[Y_k^2] = \int_0^{\infty} y^2 P_{Y_k}(y) dy \tag{15}$$

Examples of such moments are given in Section III-D. These moments are expressed in terms of the noise distribution model parameters. The parameters can be estimated from the moments computed from the measures. The association of $P_{Y_k}(y \geq 0)$ and $P_{Y_k}(y < 0)$ (for y_k^-) leads for a symmetrical noise distribution to a mean : $E[Y_{k\pm}] = \int_{-\infty}^{\infty} y P_{Y_{k\pm}}(y) dy = 0$ and a variance : $E[Y_{k\pm}^2] = \int_{-\infty}^{\infty} y^2 P_{Y_{k\pm}}(y) dy$.

Proposition 1: Y_k (corresponding to y_k^+ or/and y_k^-) is a combined variable of the original random processes N_{k-1}, N_k, N_{k+1}. Given a model P_{N_k} for N_k, it is possible to analytically or numerically calculate the corresponding model P_{Y_k} of Y_k and its various moments. These predictions can then be compared to the real measures of Y_k.

B. Estimator $NOLSE_1$ for a 1D signal

Previous sections show how the decomposition of a noisy step signal can provide a distribution of noise strongly linked to the original noise distribution. Clearly, the *pdf* of the measure Y_k is dependent on the *pdf* of the noise N_k. The moments of the observation can be defined to characterize the distribution (e.g., the two first moments). Because the signal decomposition involves derivatives, the mean of the noise cannot be estimated in the proposed approach.

Proposition 2: Using the second moment, we define the following variance estimator ($NOLSE_1$):

$$s^2 = K_2 \frac{1}{N} \sum_{k=1}^{N} y_k^2 \tag{16}$$

where K_2 is a constant ($\in \mathbb{R}^+$) depending on the assumed kind of noise and N is the size of the signal. The second moment and particularly the variance are often the most relevant characteristics for noise distributions. More generally, a p-order estimator can be defined:

$$s^p = K_p \frac{1}{N} \sum_{k=1}^{N} y_k^p \ , \ p \in \{1, 2, 3...\} \tag{17}$$

C. Quality of the estimator

The quality of the estimator $\tilde{\theta}$ of a variable θ can be characterized [11] by its bias and its *mean square error* (MSE),

$$\begin{cases} Bias\left(\tilde{\theta}\right) = E\left[\tilde{\theta}\right] - \theta \\ MSE(\tilde{\theta}) = E\left[\left(\tilde{\theta} - \theta\right)^2\right] = Var\left[\tilde{\theta}\right] + Bias\left(\tilde{\theta}\right)^2 \end{cases} \tag{18}$$

The bias of the estimator s^2 being null, its quality is measured by its variance (Var, see [14]). Let us consider now the random variable S^2 associated with the estimator s^2,

$$S^2 = K_2 \frac{1}{N} \sum_{k=1}^{N} Y_k^2$$

The variance is as follows:

$$Var\left(S^2\right) = E\left[S^4\right] - E\left[S^2\right]^2$$

and finally (see [14]),

$$Var(S^2) = K_2^2 \frac{1}{N^2} \left\{ N E[Y^4] + (2N-4) E[Y_1^2 Y_3^2] \right\}$$
$$+ K_2^2 \frac{1}{N^2} \left\{ (-5N+6) E[Y^2]^2 \right\} \tag{19}$$

This means $Var\left(S^2\right) \to 0$ as $N \to \infty$. For example, in the case of Gaussian white noise, the variance of the estimator becomes

$$Var\left(S^2\right) = \frac{8^2}{\pi^2} \frac{1}{N^2} \left\{ N \frac{2}{13} \pi^2 \sigma^4 + (2N-4) \frac{1}{41} \pi^2 \sigma^4 \right\}$$
$$+ \frac{8^2}{\pi^2} \frac{1}{N^2} \left\{ (-5N+6) \frac{1}{8^2} \pi^2 \sigma^4 \right\} \tag{20}$$

and for a long signal

$$Var\left(S^2\right) \approx \frac{8}{N} \sigma^4 \tag{21}$$

For example, the decay of the variance of the estimator of the Gaussian white noise is $1/N$ (see Figure 3).
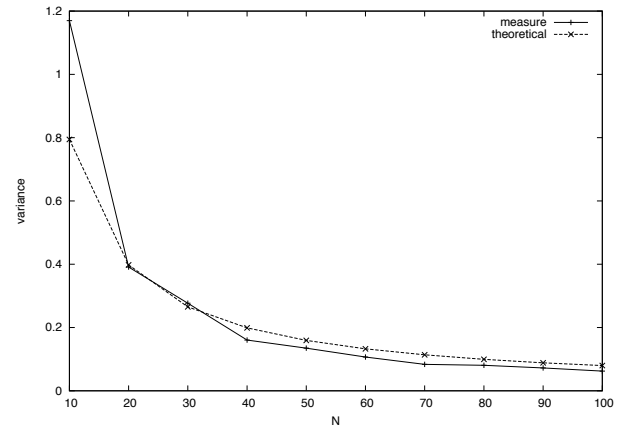

Figure 3. Variance of the (second moment) estimator with respect to different signal lengths, showing both theoretical values and experimental values (Gaussian white noise).

D. Examples of estimators for GWN and impulse noise

We propose two examples of noise estimators corresponding to two types of noise distributions: additive GWN and double exponential noise distribution.

4

1) Gaussian white noise: The *pdf* of the centered normal random variable is defined as the Gaussian function:

$$P_{N_k}(x) = \frac{1}{\sigma\sqrt{2\pi}}e^{-\frac{x^2}{2\sigma^2}} \tag{22}$$

It follows for this distribution that:

$$E\left[Y_k\right] = \pm\frac{\sigma}{2\sqrt{\pi}} \ , \quad E\left[Y_k^2\right] = \frac{\pi}{8}\sigma^2 \tag{23}$$

Proposition 3: From the above result, we define the following $NOLSE_1$ estimator s_+^2 of the variance σ^2 of the GWN:

$$s_+^2 = \frac{8}{\pi}\frac{1}{N}\sum_{k=1}^{N}(y_k^+)^2 \tag{24}$$

where N is the size of the signal and $K_2 = \frac{8}{\pi}$. Obviously, an identical estimator s_-^2 is defined for y_k^- and a mean $s^2 = \left(s_+^2 + s_-^2\right)/2$ is finally obtained for symmetric distributions,

$$s^2 = \frac{4}{\pi}\frac{1}{N}\sum_{k=1}^{N}\left(y_k^{+2} + y_k^{-2}\right) \tag{25}$$

An estimation of σ can be also obtained using an estimator based on the first moment (e.g., $s_{1+} = \frac{2}{N}\sqrt{\pi}\sum_{k=1}^{N}y_k^+$). Experimentally we verified that the variances of S^2 and $(S_1)^2$ are similar for the corresponding Gaussian distribution.

2) Impulse or double exponential noise distribution: We make reference to the impulse noise with a double exponential noise distribution defined by the *pdf*:

$$P_{N_k}(x) = \frac{1}{2\beta}e^{-\frac{|x|}{\beta}} \tag{26}$$

where:

$$\begin{cases} \int_{-\infty}^{\infty} P_{N_k}(x)dx = 1 \\ E\left[X_k^2\right] = \int_{-\infty}^{\infty} x^2 P_{N_k}(x)dx = 2\beta^2 \end{cases} \tag{27}$$

Considering the random variable Y_k associated with the noise component y_k^+ in Eq. 9 (or y_k^-), we deduce the following:

$$P_{Y_k}(y) = \begin{cases} \frac{1}{12\beta}\left(-2e^{-\frac{2}{\beta}y} + 5e^{-\frac{y}{\beta}}\right) & y > 0 \\ \frac{2}{3} & y = 0 \\ 0 & y < 0 \end{cases} \tag{28}$$

$$E\left[Y_k\right] = \pm\frac{3}{8}\beta \ , \quad E\left[Y_k^2\right] = \frac{3}{4}\beta^2 \tag{29}$$

Proposition 4: A $NOLSE_1$ estimator of the parameter β for the double exponential distribution is defined as follows:

$$s_{\beta+} = \frac{8}{3}\frac{1}{N}\sum_{k=1}^{N}y_k^+ \tag{30}$$

$K_1 = \frac{8}{3}$ and the mean estimator is : $s_\beta = (s_{\beta+} + s_{\beta-})/2$ where $s_{\beta-} = -\frac{8}{3}\frac{1}{N}\sum_{k=1}^{N}y_k^-$.
Another estimator can be defined on the basis of the second moment. We verify experimentally that the variances of the estimators for the double exponential distribution are similar.

IV. 1D PERFORMANCE

The performance of the $NOLSE_1$ estimator is studied for a synthetic signal and noise (additive GWN). The influences of edge density and point correlation are also simulated. Finally, a typical noise distribution (double exponential) is also tested, and the $NOLSE_1$ performance is compared to the MAD (Median Absolute Deviation) estimate (one of the most commonly used noise estimator and renowned for being one of the best).

A. Methods for comparison

As discussed in the introduction, we chose to compare the proposed method with the MAD estimate,

$$s_{MAD}^2 = \left(\frac{\text{median}(|d|)}{0.6745}\right)^2 \tag{31}$$

where d is the first detail level of the wavelet analysis with the Haar wavelet. The two methods share the same elementary derivatives used to estimate the noise. We also use the MSE measurement as a reference, if possible.

B. Influence of the edge density and the edge model on the estimator (GWN)

The highest edge density in a discrete unit step edge model corresponds to the following pattern: 0011 where the length L_P is 4. We then define the edge density by:

$$D = \frac{4}{L_P} \tag{32}$$

The details of this section and a theoretical study of the influence of a more realistic edge signal can be found in the report [14] (section 2.2). The variance with respect to the edge amplitude for $NOLSE_1$ and MAD are compared in Fig 4. The maximum bias of $NOLSE_1$ is approximately 27%. This value is smaller for a realistic edge model at 15% . There is no upper bound for the MAD estimator (however, a limit exists due to the bounded signal amplitude).

Figure 5 shows the favorable performance of $NOLSE_1$ when the edge density increases and also demonstrates the sensitivity of MAD to edges. The line of the results of Figure 5 leads to (for $D \in]0,1]$):

$$\begin{cases} variance \approx 0.986 + 0.248 \times D & \text{for } MAD \\ variance \approx 1.008 + 0.058 \times D & \text{for } NOLSE_1 \end{cases}$$

We show in the report [14] that while the influence of the edge is limited, it is not negligible for a high edge density. However, in most real signals or images, the edge density is not extremely high, and the extended edges counterbalance this influence. In the case of high amplitudes ($A > \sigma$), the estimate could be corrected by eliminating measures with high edge amplitudes.
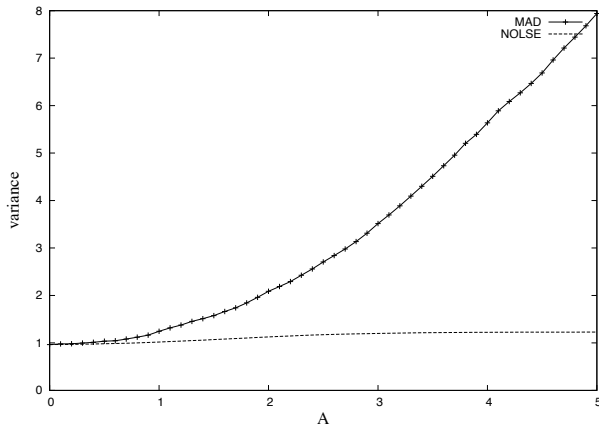
Figure 4. MAD and $NOLSE_1$ variance estimates according to the edge amplitude A for the discrete periodic signal $00AA00AA...$ (highest density $D = 1$, $\sigma^2 = 1$). $NOLSE_1$ is particularly robust (Gaussian white noise).
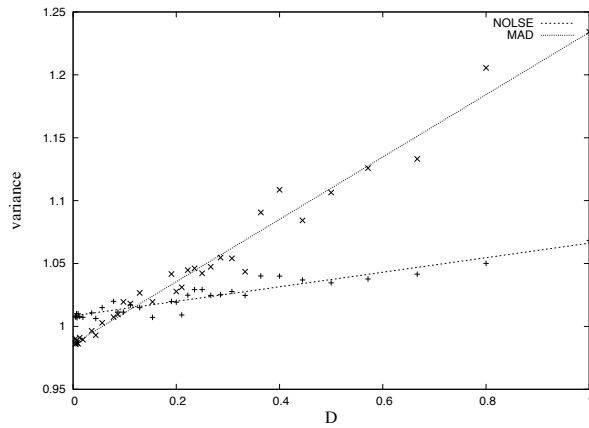

Figure 5. MAD and $NOLSE_1$ variance estimate for the discrete periodic signal $00AA00AA...$ ($A = 1$, $\sigma^2 = 1$) with respect to the edge density (Gaussian white noise).

V. 2D EXTENSION AND APPLICATIONS

This section proposes a 2D extension of the $NOLSE$ estimator. The performance of the $2D$ estimator ($NOLSE_2$) is evaluated with several models and noise distributions. The following images (size: 256×256 or 512×512) are used to evaluate the performance: *Barbara*, *Boat*, *House*, *Lena* and *Office* (see Figure 6). In this part, we denote the estimators with the Greek letter ς and, in particular, the second moment estimator with ν. We continue to refer to the 1D estimator by the letter s. ν_{MAD} is the variance obtained using the 2D-version of the MAD estimator, and σ^2 or v remains as the Gaussian noise variance. The MSE measure (between the original image and the noisy image), ν_{MSE}, will be presented as an indicative value for real images because these images are not free from noise (this noise being more or less correlated). We introduce two efficient methods for additional comparisons. One is based on the image convolution with the Laplacian operator [9] ($FNVE$), and the other is the corresponding refinement with edge detection [29] (TY). These methods are not iterative and are more or less comparable with MAD and $NOLSE$ in algorithm complexity.

Figure 6. Test images: *Barbara*, *Boat*, *House*, *Lena* and *Office*.

A. Algorithm

Because the approach is based on the first derivative, certain particular edge configurations can be seen as noise, and this is the case for lines in an image or, more generally, for roof profiles oriented in any direction. Most of these issues can be avoided by extending the 1D algorithm along the two main directions of the images. For each pixel $I(i, j)$, the directional noise components (the derivatives along the horizontal and vertical directions) are computed. Defining the directional operators $D_i^{R+}, D_j^{R+}, D_i^{R-}, ...$ a first measure of the noise is established as follows:

$$\begin{cases} y_j^+ = \min\left(D_j^{L+}\left(I\right), -D_j^{R-}\left(I\right)\right) \\ y_1 = \min\left(D_i^{L+}\left(y_j^+\right), -D_i^{R-}\left(y_j^+\right)\right) \quad y_{1 \geq 0} \end{cases} \quad (33)$$

The variable y_1 is obtained by consecutively applying the directional operators along the lines (intermediate result y_j^+) and then along the columns. Other measures such as y_2, y_3, y_4 can be obtained as follows:

$$\begin{cases} y_j^- = -\min\left(-D_j^{L-}\left(I\right), D_j^{R+}\left(I\right)\right) \\ y_2 = -\min\left(-D_i^{L-}\left(y_j^-\right), D_i^{R+}\left(y_j^-\right)\right) \quad y_2 \leq 0 \end{cases} \quad (34)$$

$$\begin{cases} y_i^+ = \min\left(D_i^{L+}\left(I\right), -D_i^{R-}\left(I\right)\right) \\ y_3 = \min\left(D_j^{L+}\left(y_i^+\right), -D_j^{R-}\left(y_i^+\right)\right) \quad y_3 \geq 0 \end{cases} \quad (35)$$

$$\begin{cases} y_i^- = -\min\left(-D_i^{L-}\left(I\right), D_i^{R+}\left(I\right)\right) \\ y_4 = -\min\left(-D_j^{L-}\left(y_i^-\right), D_j^{R+}\left(y_i^-\right)\right) \quad y_4 \leq 0 \end{cases} \quad (36)$$

Proposition 5: $\{y_n\}_{n=1,2,3,4}$ are measures of the noise distribution in the image. A p order estimator ς_n^p on the measures y_n can generally be defined as:

$$\varsigma_n^p = K_p \frac{1}{N} \sum_{k=1}^{N} y_{n,k}^p \ , \ p \in \{1, 2, 3...\} \quad (37)$$

where $K_p \in \mathbb{R}$ and N is the number of pixels. $\{y_n\}_{n=1,3}$ and $\{y_n\}_{n=2,4}$ can be used to estimate asymmetrical distributions.

B. GWN in images

Proposition 6: For a Gaussian white noise, the set of estimators for an input variance σ^2 is ($K_2 = 4$):

$$\left\{\nu_n = 4\frac{1}{N} \sum_{k=1}^{N} y_{n,k}^2\right\}_{n=1,2,3,4} \quad (38)$$

The mean estimator of the variance for symmetrical distribution of Gaussian noise is as follows:

$$\nu = \sum_{n=1}^{4} \frac{1}{N} \sum_{k=1}^{N} y_{n,k}^2 \quad (39)$$

6

Tables I, II, III, IV, and V, present comparison results for MAD, $FNVE$, TY and $NOLSE_2$, respectively. Except for zero noise (natural noise only) or low level of noise, the different methods give similar and satisfactory results.

When noise is added, the measure of the natural noise is deducted from the new measure. Depending on the image, $NOLSE_2$ leads to rather different results because it is sensitive to fine textures and generally overestimates the noise level. MAD gives values depending on the image quantification, $FNVE$ over-estimates the noise level and TY slightly underestimates the noise level. In the case of additive Gaussian noise, the TY method seems to yield the most reliable results.

Table I
ESTIMATES OF DIFFERENT GWN LEVELS (σ_{added}). THE ESTIMATES OBTAINED FOR THE ORIGINAL IMAGE ($\tilde{\sigma}_{added} = 0 \rightarrow \tilde{\sigma}_{image}$) ARE USED TO COMPUTE $\tilde{\sigma}_{added} = \tilde{\sigma} - \tilde{\sigma}_{image}$..

Barbara (512×512) image : noise estimates of σ_{added}			
σ_{added}	MAD	$FNVE$	TY	$NOLSE_2$
0.00	3.71	4.96	**2.28**	8.57
2.00	2.60	2.58	2.30	**1.78**
5.00	5.98	5.87	5.48	**4.63**
9.98	11.25	10.88	10.65	**9.57**
15.05	16.44	15.83	15.86	**14.52**
20.06	21.51	20.80	20.64	**19.62**

Table II
ESTIMATES OF DIFFERENT GWN LEVELS (σ_{added}). THE ESTIMATES OBTAINED FOR THE ORIGINAL IMAGE ($\tilde{\sigma}_{added} = 0 \rightarrow \tilde{\sigma}_{image}$) ARE USED TO COMPUTE $\tilde{\sigma}_{added} = \tilde{\sigma} - \tilde{\sigma}_{image}$.

Boat image : noise estimates of σ_{added}			
σ_{added}	MAD	$FNVE$	TY	$NOLSE_2$
0.00	2.22	3.00	**1.06**	4.08
2.00	2.95	2.41	**2.16**	1.84
5.04	6.03	5.46	**5.15**	4.77
9.97	10.90	10.44	**10.09**	9.71
14.99	15.71	15.38	**14.90**	14.56
20.01	20.71	20.40	20.48	**19.63**

Table III
ESTIMATES OF DIFFERENT GWN LEVELS (σ_{added}). THE ESTIMATES OBTAINED FOR THE ORIGINAL IMAGE ($\tilde{\sigma}_{added} = 0 \rightarrow \tilde{\sigma}_{image}$) ARE USED TO COMPUTE $\tilde{\sigma}_{added} = \tilde{\sigma} - \tilde{\sigma}_{image}$..

House image : noise estimates of σ_{added}			
σ_{added}	MAD	$FNVE$	TY	$NOLSE_2$
0.00	2.22	1.69	**0.97**	1.87
2.00	**1.96**	2.11	2.06	1.87
4.98	5.18	5.16	**4.99**	4.86
10.02	**10.01**	10.17	9.97	9.78
15.00	15.07	15.19	**14.98**	14.78
20.03	20.38	20.49	20.72	**20.02**

Table IV
ESTIMATES OF DIFFERENT GWN LEVELS (σ_{added}). THE ESTIMATES OBTAINED FOR THE ORIGINAL IMAGE ($\tilde{\sigma}_{added} = 0 \rightarrow \tilde{\sigma}_{image}$) ARE USED TO COMPUTE $\tilde{\sigma}_{added} = \tilde{\sigma} - \tilde{\sigma}_{image}$..

Lena image : noise estimates of σ_{added}			
σ_{added}	MAD	$FNVE$	TY	$NOLSE_2$
0.00	1.48	2.64	**1.10**	3.71
2.00	2.72	2.45	**2.10**	1.83
5.00	5.82	5.48	**5.09**	4.69
9.97	10.71	10.54	**10.26**	**9.68**
15.03	15.92	15.53	**14.98**	14.73
20.09	20.61	20.50	**20.10**	19.70

Table V
ESTIMATES OF DIFFERENT GWN LEVELS (σ_{added}). THE ESTIMATES OBTAINED FOR THE ORIGINAL IMAGE ($\tilde{\sigma}_{added} = 0 \rightarrow \tilde{\sigma}_{image}$) ARE USED TO COMPUTE $\tilde{\sigma}_{added} = \tilde{\sigma} - \tilde{\sigma}_{image}$..

Office image : noise estimates of σ_{added}			
σ_{added}	MAD	$FNVE$	TY	$NOLSE_2$
0.00	**0.74**	1.31	1.30	1.12
2.00	2.39	2.23	1.74	**1.88**
5.01	5.38	5.20	**4.90**	4.74
10.02	10.26	10.22	**9.98**	9.63
14.95	15.11	15.22	**14.93**	14.54
19.92	19.86	20.08	**19.91**	19.39

deviation parameter σ. Multiplicative noise can be seen as an approximation of the image sensor response because the noise level in the CCD and CMOS camera increases as the luminance increases [5].

Proposition 7: In the case of speckle noise (multiplicative noise) the effective noise variance ν_{MSE} can be estimated by the Gaussian noise estimator: $\nu_{NOLSE_2} = \nu$, ν is given by Eq. 39.

Table VI
PERFORMANCES OF SPECKLE NOISE FOR THE *Office* IMAGE: ν CORRESPONDS TO $NOLSE_2$ AND ν_{MSE} IS THE MEASURED NOISE VARIANCE (THE MSE OF THE DIFFERENCE BETWEEN THE ORIGINAL IMAGE AND ITS NOISY VERSION). THIS NOISE VARIANCE DOES NOT INCLUDE THE UNKNOWN INITIAL NOISE OF THE IMAGE. ν ($NOLSE_2$) IS A RELIABLE ESTIMATOR AND s^2 CORRESPONDS TO EQ 25(1D ESTIMATOR).

$10^3\nu$	0	0.0005	0.001	0.005	0.01	0.05	0.1
ν_{MSE}	0	0.086	0.171	0.849	1.65	7.79	14.7
ν_{MAD}	**0.008**	0.073	0.111	0.359	0.636	2.56	4.74
ν_{FNVE}	0.026	0.100	0.164	0.669	1.23	5.66	10.5
ν_{TY}	0.026	**0.096**	0.158	0.639	1.17	5.39	9.96
ν_{NOLSE_2}	0.020	0.097	**0.176**	**0.807**	**1.57**	**7.79**	**14.5**
s^2_{NOLSE}	0.315	0.391	0.469	1.08	1.85	7.90	14.5

C. Speckle noise

The result J of multiplicative noise in an image is defined as:

$$J = I + \sigma.\eta.I$$

where I is the original image, and η is a normalized Gaussian noise distribution with a mean equal to 0 and a standard

Table VII
SPECKLE NOISE ESTIMATION FOR SELECTED NOISED REAL IMAGES WITH SIMILAR NOISE LEVELS (ν_{MSE}). THE NOISE PARAMETER IS $\nu = \sigma^2$.

Image	Barbara	Boat	House	Lena	Office
$10^3\nu$	0.0025	0.0029	0.0023	0.00285	0.005
ν_{MSE}	0.839	0.849	0.826	0.835	0.849
ν_{MAD}	1.798	1.064	**0.825**	0.964	0.359
ν_{FNVE}	4.265	1.047	0.884	1.010	0.669
ν_{TY}	**1.382**	0.533	0.745	**0.746**	0.639
$NOLSE_2$	8.013	**1.046**	0.845	1.003	**0.807**

7

Table VI shows the performance of $NOLSE_1$ and $NOLSE_2$ for speckle noise. Except in cases of low noise levels, in which the initial noise and/or certain edge points can explain the small difference between the real noise (ν_{MSE}) and that estimated by $NOLSE_2$, the results are correct. Note that MAD is not efficient because the noise level varies with respect to the luminance level. For strong noise levels, the edges become negligible, and $NOLSE_1$ (s^2) gives similar results to $NOLSE_2$ (ν). The other methods ($FNVE$, TY) underestimate the noise level because they measure the low amplitudes which is a problem in the case of multiplicative noise. For moderate noise levels, table VII shows that the estimation accuracy for all the proposed techniques depends on the images. In textured images like Barbara, the noise estimation is nearly impossible whatever the method. Figure 7
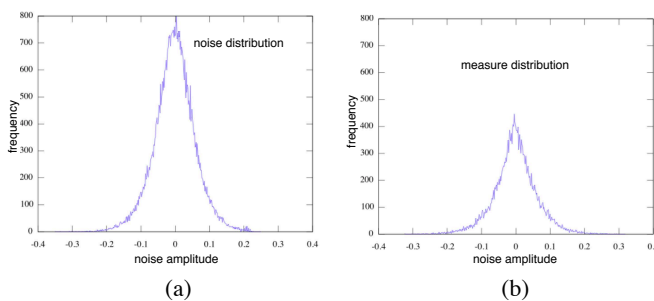

Figure 7. Speckle noise distribution ($\sigma^2 = 0.01$) in the *House* image. Left: true noise distribution. Right: distribution of the measures: y_1 (right part: positive amplitudes; see Eq. 33) and y_2 (left part: negative amplitudes; see Eq. 34). $\nu_{MSE} = 0.0035$, $\nu_{MAD} = 0.0028$, $s^2 = 0.0036$, $\nu = 0.0035$.

presents an example of the speckle noise distribution (level $\sigma^2 = 0.01$) in the *House* image and the distribution obtained from measures y_1 and y_2 defined in Eqs. 33 and 34. The y_1 measure corresponds to the right part of the distribution (positive amplitudes) and the y_2 measure corresponds to the left part.

D. Salt-and-pepper noise

Proposition 8: In the case of salt-and-pepper noise with a noise level d (%), the effective noise variance ν_{MSE} can be estimated on the basis of the Gaussian noise estimator:

$$\nu_I = \kappa.\nu^\gamma \qquad (40)$$

where:

$$\begin{cases} \kappa & \simeq 1.20 \\ \gamma & \simeq 1.22 \\ \nu & \text{is given by Eq. 39} \end{cases} \qquad (41)$$

The coefficients are empirically deduced from experimental tests on a constant image with a gray level equal to 0.5. The estimator leads to $\nu = \nu_+ + \nu_-$ with $\nu_+ = (\nu_1 + \nu_3)/4$ and $\nu_- = (\nu_2 + \nu_4)/4$. Defining $\nu_I = \nu_{I+} + \nu_{I-}$ and developing the Taylor expression of ν_I to first order around the mean $\nu/2$

Table VIII
PERFORMANCE FOR THE SALT-AND-PEPPER NOISE (d DENSITY PARAMETER) FOR THE *Office* IMAGE. ν_I CORRESPONDS TO $NOLSE_2$ (EQ. 40), AND ν_{MSE} IS THE MEASURED NOISE VARIANCE (THE MSE ON THE DIFFERENCE BETWEEN THE ORIGINAL IMAGE AND ITS NOISY VERSION). ν_I IS A RELIABLE ESTIMATOR. ν_{I+} AND ν_{I-} GIVE A GOOD APPROXIMATION OF THE NOISE COMPONENTS FOR THE SALT AND PEPPER IMPULSES, RESPECTIVELY.

d (%)	0	5	10	20	40
ν_{MSE}	0.000	0.018	0.036	0.071	0.143
ν_{MAD}	0.000	0.000	0.000	0.002	0.112
ν_{FNVE}	0.000	0.006	0.020	0.055	0.124
ν_{TY}	0.000	0.006	0.019	0.012	0.077
ν_I	0.000	**0.018**	**0.038**	**0.079**	**0.146**
ν_{MSE+}	0.000	0.013	0.026	0.050	0.100
ν_{MSE-}	0.000	0.005	0.010	0.021	0.042
ν_{I+}	0.000	0.013	0.029	0.055	0.093
ν_{I-}	0.000	0.004	0.010	0.023	0.053

Table IX
PERFORMANCE FOR THE SALT-AND-PEPPER NOISE (d DENSITY PARAMETER) FOR SELECTED REAL IMAGES. ν_I CORRESPONDS TO $NOLSE_2$ (EQ. 40), AND ν_{MSE} IS THE MEASURED NOISE VARIANCE (THE MSE ON THE DIFFERENCE BETWEEN THE ORIGINAL IMAGE AND ITS NOISY VERSION). ν_I IS A RELIABLE ESTIMATOR. ν_{I+} AND ν_{I-} GIVE A GOOD APPROXIMATION OF THE NOISE COMPONENTS FOR THE SALT AND PEPPER IMPULSES, RESPECTIVELY.

Image	Barbara	Boat	House	Lena	Office
d (%)	10	10	10	10	10
ν_{MSE}	0.030	0.028	0.029	0.028	0.036
ν_{MAD}	0.004	0.001	0.000	0.000	0.000
ν_{FNVE}	0.026	0.019	0.019	0.019	0.020
ν_{TY}	0.006	0.003	0.003	0.003	0.019
ν_I	**0.031**	**0.027**	**0.029**	**0.028**	**0.038**
ν_{MSE+}	0.016	0.014	0.011	0.014	0.026
ν_{MSE-}	0.014	0.015	0.018	0.014	0.010
ν_{I+}	0.017	0.013	0.011	0.013	0.029
ν_{I-}	0.014	0.014	0.019	0.014	0.010

gives the following:

$$\begin{aligned} \nu_I &= \kappa.(\nu_+ + \nu_-)^\gamma \\ &= \kappa\left(\frac{\nu}{2} + \left(\nu_+ - \frac{\nu}{2}\right) + \frac{\nu}{2} + \left(\nu_- - \frac{\nu}{2}\right)\right)^\gamma \\ &\simeq \kappa\left(\frac{\nu^\gamma}{2}.(1 - \gamma) + \gamma\nu^{\gamma-1}\nu_+\right) \\ &\quad + \kappa\left(\frac{\nu^\gamma}{2}(1 - \gamma) + \gamma\nu^{\gamma-1}\nu_-\right) \end{aligned}$$

We identify this expression with

$$\nu_I = \nu_{I+} + \nu_{I-} \qquad (42)$$

and it follows that

$$\begin{cases} \nu_{I+} = & \kappa\left(\frac{\nu^\gamma}{2}(1 - \gamma) + \gamma\nu^{\gamma-1}\nu_+\right) \\ \nu_{I-} = & \kappa\left(\frac{\nu^\gamma}{2}(1 - \gamma) + \gamma\nu^{\gamma-1}\nu_-\right) \end{cases} \qquad (43)$$

Table VIII presents variance estimates of the *Office* image. The estimator ν_I gives satisfactory results. The second part of the table shows the ability of the measures to provide a good estimate of the positive (salt) and negative (pepper) impulses of the noise. The estimate quality decreases as the noise density increases because the 2D algorithm cannot always correctly separate the positive and negative impulses that are similar

8

to each other. The MAD is again not as effective on this nonlinear (and non-additive) noise. Table IX confirms the reliability of $NOLSE$ whatever the image.

E. Poisson noise

This noise distribution typically models shot noise in a sensor in which the time between photon arrivals is governed by Poisson statistics [4], [8]. Defining the expected number of occurrences by the integer λ (e.g., proportional to the number of electrons created during photon acquisition), the probability of the noise corresponds to observing the number n instead of λ at the pixel k:

$$P_{\lambda_k}(n) = \frac{\lambda^n e^{-\lambda}}{n!} \tag{44}$$

The Poisson distribution is characterized by $E[n] = \lambda$ and $Var[n] = \lambda$. Table X summarizes selected results on synthetic images, and Table XI presents tests on real images.

Proposition 9: In the case of Poisson noise, the variance λ can be estimated at first approximation by the Gaussian noise estimator : $\lambda_{NOLSE_2} = \nu$ (ν is given by Eq. 39)

Table X
EXAMPLES OF POISSON NOISE ESTIMATION FOR A SYNTHETIC IMAGE COMPOSED OF TWO UNIFORM AREAS (SIZE 128×64) WITH GRAY LEVELS L_1 AND L_2. IT FOLLOWS THAT THE POISSON NOISE IS GENERATED ACCORDING TO THE TWO PARAMETERS $\lambda_1 = L_1$ AND $\lambda_2 = L_2$.

λ_1 measured λ_2	102 0	100 10	100 30	101 59	99 102
$\lambda = (\lambda_1 + \lambda_2)/2$	51	55	65	80	100
λ_{MAD}	0	27	55	**79**	108
λ_{FNVE}	26	45	62	83	109
λ_{TY}	24	15	44	78	**103**
λ_{NOLSE_2}	**48**	**53**	**64**	82	**103**

Table XI
POISSON NOISE ESTIMATION FOR SELECTED REAL IMAGES. THE NOISY IMAGE VERSION IS I_P.

Image	Barbara	Boat	House	Lena	Office
$MSE(I_p - I)$	117	130	138	124	91
MAD	204	141	140	141	47
$FNVE$	358	144	142	138	72
TY	**201**	101	125	117	68
$NOLSE_2$	522	**140**	**137**	**131**	**83**

The results show the ability of $NOLSE_2$ to measure the variance of the Poisson distribution. Because a distribution measure is available, the noise can be estimated by regions in the image (the variance varies according to the signal amplitude) at the cost of accuracy. All the techniques fail to estimate the Poisson noise on heavily textured images like Barbara.

The perspective study on multiplicative noise will consider the distribution analysis and its moments.

F. Advantages and limitations of the approach

The different studies in the above sections highlight the ability of the approach to estimate the noise level for various noise distributions and models (additive and multiplicative).

Unlike many of the approaches that are based on low amplitudes to avoid edge information, the $NOLSE$ approach attempts to separate the noise from the edge information regardless of the edge amplitude. This principle allows for correct noise estimation even in multiplicative models in which the noise level increases with the edge amplitude. Concerning the limitations, because the approach is based on the step edge model, measuring the local peak information at the edge is therefore considered as noise and limits the universality of the approach. The 2D extension remains directional because it performs the derivatives in the two directions. Lines and textures in any direction can therefore be interpreted partially or completely as noise components. Figure 8 illustrates these limitations in which the fine texture (1 pixel width) is interpreted as noise. Other 2D schemes can be defined,
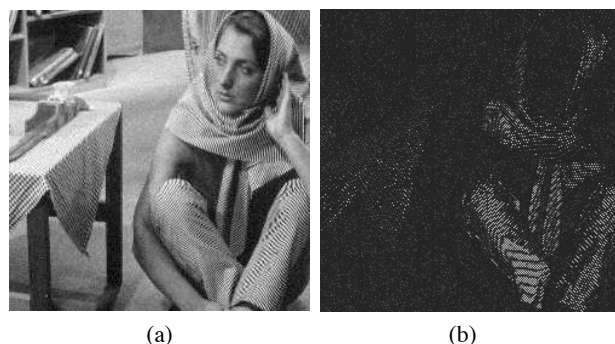

(a)   (b)

Figure 8. Example of the limitations of the approach for the image "Barbara" (size 256×256, normalized to 1 before addition of noise). (a) noisy image (GWN $\sigma^2 = 0.001$); (b) measures of y_1. The highlighted fine texture (1-pixel width) areas are detected by the y_1 estimator.

for example, by combining the 1D detection of positive and negative peaks. However, while the selectivity against edge points increases, the detection decreases and the variance of the estimator increases. In contrast, the approach permits the definition of bi-directional derivatives (by including the diagonal directions). Further work involving applications to pattern analysis, particularly in edge detection for specific image topologies and texture analysis is needed to validate this generalization.

VI. CONCLUSION

This work introduces a method for estimating the main parameters of a noise distribution. Using this method, it is possible to estimate the noise distribution from the measured distribution. The method is defined in the discrete domain and is based on a step model signal; however, it is also valid for more realistic extended profiles. The model does not make assumptions regarding the distribution of the noise and is able to measure additive noise as well as multiplicative noise, salt-and-pepper noise and Poisson noise, which proves that the approach described by the method is not limited to additive noise models. To estimate non-additive noise, it is not necessary to transform the image; on the contrary, in order to deduce the noise parameter it is sufficient to know the correct estimator. The asymmetry of the noise distribution can be accurately estimated if the noise distribution is not dense, as in the case of salt-and-pepper noise. The complexity of the

algorithm is low, and its implementation should not present difficulties in any computing language. Additionally, it can be integrated into hardware camera circuits for real-time systems.

However, the approach suffers from certain limitations. It does not completely eliminate the edge points in 2D because it is sensitive to fine textures (1D pixel width), and this seems to limit the accuracy of $NOLSE_2$ in the case of natural noise. The theoretical pdf is not easy to calculate for any noise distribution; however, numerical solutions can be found.

The perspectives offered by this approach are numerous. We are currently working on a refined noise estimation for GWN based on its pdf approximation. Further work is required to extend the applications. The study of camera models using several noise distributions particularly the most frequently encountered Poisson distribution [5] is in progress. The generalization of the polarized derivatives to the bi-directional derivative has been introduced. Applications to texture analysis, edge detection (edge detection can be also used to refine the noise estimate) and analysis of specific topology (e.g., images from catadioptric systems) and 3D images will be considered. Finally, it may be of interest to define noise measures for other signal models and to focus on local noise estimation.

REFERENCES

[1] R. Bracho and A.C. Sanderson. "Segmentation of images based on intensity gradient information". In *Conf. on Computer Vision and Pattern Recognition*, pp. 341–347, 1985.

[2] A. Buades, B. Coll, and J. M. Morel. "A review of image denoising algorithms, with a new one". *Multiscale Modeling and Simulation*, Vol. 4, No. 2., pp. 490–530. 2005.

[3] J. Canny. A computational approach to edge detection. *IEEE Trans. Pattern Anal. and Machine Intell.*, vol. 8, no. 6, pp. 679–698, Nov. 1986.

[4] Kodak Company. "CCD Image Sensor Noise Sources". Technical report, Image sensor solution / Application note, www.kodak.com/go/imagers, 2005.

[5] R. Costantini and S. Süsstrunk. Virtual Sensor Design. In *Proc. IS&T/SPIE Electronic Imaging 2004: Sensors and Camera Syst. for Scientific, Indus., and Digital Photography Appli. V*, volume 5301, pages 408–419, 2004.

[6] D. Donoho. "De-noising by soft-thresholding". *IEEE Trans. Inf. Theory*, 41, pp. 613–627, 1995.

[7] D. Donoho and I. Johnstone. "Ideal spatial adaptation via wavelet shrinkage". *Biometrika*, 81, pp. 425–455, 1994.

[8] A. Foi, M. Trimeche, V. Katkovnik, and K. Egiazarian. "Practical poissonian-gaussian noise modeling and fitting for single-image raw-data". *IEEE Trans. Image Processing*, pp. 1737-1754, Vol. 17, no. 10, 2008.

[9] J. Immerkær. "Fast Noise Variance Estimation". "*Computer Vision and Image Understanding*", pp. 300–302, Vol. 64, no. 2, Sept. 1996.

[10] A. Jalobeanu, L. Blanc-Féraud, and J. Zerubia. Estimation of blur and noise parameters in remote sensing. In *In Proc. of Int. Conf. on Acoustics, Speech and Signal Processing*, pages 249–256, 2002.

[11] S. M. Kay. *Fundamentals of Statistical Signal Processing*. Prentice Hall, 1993.

[12] H. Krim, D. Tucker, and S. Mallat. "On denoising and best signal representation". *IEEE Trans. Inf. Theory*, vol. 45, no 7, pp. 2225–2238, 1999.

[13] O. Laligant and F. Truchetet. "A nonlinear derivative scheme applied to edge detection". *IEEE Trans. Pattern Anal. and Machine Intell.*, 32 (2):242–257, 2010.

[14] O. Laligant, F. Truchetet, and E. Fauvet. "The noise estimator NOLSE". Technical report, Le2i Lab. / University of Burgundy, April 2012.

[15] G. Landi and E. Loli Piccolomini. An algorithm for image denoising with automatic noise estimate. *J. Math. Imaging Vis.*, 34:98–106, May 2009.

[16] F.-X. Lapalme, A. Amer, and C. Wang. "FPGA architecture for real-time video noise estimation". In *Inter. Conf. on Image Processing*, pp. 3257–3260, 2006.

[17] C. Liu, W. T. Freeman, R. Szeliski, and S. Bing Kang. "Noise estimation from a single image". *IEEE Conf. Computer Vision and Pattern Recognition*, vol. 1, pp. 901–908, Mar. 2006.

[18] C. Liu, R. Szeliski, S. Bing Kang, C. L. Zitnick, and W. T. Freeman. Automatic estimation and removal of noise from a single image. *IEEE Trans. Pattern Anal. and Machine Intell.*, 30(2):299–314, 2008.

[19] Mairal, M. Elad, and G. Sapiro. "Learning multiscale sparse representations for image and video restoration,". *IEEE Trans. Image Processing*, pp. 53-69, Vol. 17, no. 1, 2008.

[20] P. Meer, J.M. Jolion, and A. Rosenfeld. "A fast algorithm for blind estimation of noise variance". *IEEE Trans. Pattern Anal. and Machine Intell.*, vol. 12, no 2, pp. 216–223, 1990.

[21] M. Motwani, M. Gadiya, R. Motwani, and Jr. F. C. Harris. "A Survey of Image Denoising Techniques". In *Proceedings of GSPx 2004, Santa Clara Convention Center, Santa Clara, CA*, September 27–30 2004.

[22] S. I. Olsen. "Noise Variance Estimation in Images". In *Proc. 8th SCIA*, pages 25–28, 1993.

[23] P. Perona and J. Malik. "Scale space and edge detection using anisotropic diffusion". *IEEE Trans. Pattern Anal. and Machine Intell.*, Vol. 12, pp. 629–639. 1990.

[24] H. Sari-Sarraf and D. Brzakovic. "Automated Iterative Noise Filtering. *IEEE Trans. Signal Processing*, vol. 39, no 1, pp. 238–242, 1991.

[25] S. M. Smith and J. M. Brady. "SUSAN - a new approach to low level image processing". *Int. J. Comput. Vis.*, 23, pp. 45–78, 1997.

[26] C. Staelin and H. Nachlieli. "Image noise estimation using color information". Technical report, Hewlett-Packard Development Company, 2007.

[27] J. Starck, E. Candès, and D. Donoho. "The curvelet transform for image denoising". *IEEE Trans. Image Processing*, 11, pp. 670–684, 2000.

[28] A. Stefano, P. White, and W. Collis. "Training methods for image noise level estimation on wavelet components". *EURASIP Journal on Applied Signal Processing*, 16:2400–2407, 2005.

[29] S.-C. Tai and S.-M. Yang. "A Fast Method For Image Noise Estimation Using Laplacian Operator and Adaptive Edge Detection". "*ISCCSP*", pp. 1077–1081, March 2008.

[30] C. Tomasi and R. Manduchi. "Bilateral filtering for gray and color images". In *In Proc. IEEE Int. Conf. Computer Vision*, pp. 839–846, 1998.

[31] D. Tschumperlé and L. Brun. "Image Denoising and Registration by PDE's on the Space of Patches". In *International Workshop on Local and Non-Local Approximation in Image Processing (LNLA'08), Lausanne, Suisse*, pages 32–40, 2008.

[32] H. Vorhees and T. Poggio. "Detection textons and textures boundaries in natural images". In *Inter. Conf. on Computer Vision*, pp. 250–258, 1987.

[33] A. B. Watson, G. Y. Yang, J. A. Solomon, and J. Villasenor. "Visibility of Wavelet Quantization Noise". *IEEE Trans. Image Processing*, pp. 1164–1175, Vol. 6, no. 8, Aug. 1997.

[34] P. Wyatt and H. Nakai. "Developping Nonstationary Noise Estimation for Application in Edge and Corner Detection". *IEEE Trans. Image Processing*, pp. 1840–1853, Vol. 16, no. 7, July 2007.

Olivier Laligant received his PhD degree in 1995 from the Université de Bourgogne, France. He is full professor in the computing, electronic, imaging department (Le2i) at Université de Bourgogne, France. His research interests are focused on image analysis, edge detection, nonlinear regularization, and noise estimation.

Frédéric Truchetet received the master degree in physics at Dijon University, France, in 1973 and a PhD in electronics at the same university in 1977. He is full professor at Le2i. His research interests are focused on image processing for artificial vision inspection and particularly on wavelet transforms, multiresolution edge detection, and image compression.

Eric Fauvet received his PhD degree in 1990 in electronic and image processing from the University of Burgundy, France. He is lecturer in the Le2i laboratory of the University of Burgundy since 1990. His research interests includes signal and image processing, stochastic optimization, and pattern recognition.